OPTICS

Direct Kerr frequency comb atomic spectroscopy and stabilization

Liron Stern[1,2]*, Jordan R. Stone[1,2], Songbai Kang[1,2], Daniel C. Cole[1,2], Myoung-Gyun Suh[3], Connor Fredrick[1,2], Zachary Newman[1,2], Kerry Vahala[3], John Kitching[1], Scott A. Diddams[1,2], Scott B. Papp[1,2]*

Microresonator-based soliton frequency combs, microcombs, have recently emerged to offer low-noise, photonic-chip sources for applications, spanning from timekeeping to optical-frequency synthesis and ranging. Broad optical bandwidth, brightness, coherence, and frequency stability have made frequency combs important to directly probe atoms and molecules, especially in trace gas detection, multiphoton light-atom interactions, and spectroscopy in the extreme ultraviolet. Here, we explore direct microcomb atomic spectroscopy, using a cascaded, two-photon 1529-nm atomic transition in a rubidium micromachined cell. Fine and simultaneous repetition rate and carrier-envelope offset frequency control of the soliton enables direct sub-Doppler and hyperfine spectroscopy. Moreover, the entire set of microcomb modes are stabilized to this atomic transition, yielding absolute optical-frequency fluctuations at the kilohertz level over a few seconds and <1-MHz day-to-day accuracy. Our work demonstrates direct atomic spectroscopy with Kerr microcombs and provides an atomic-stabilized microcomb laser source, operating across the telecom band for sensing, dimensional metrology, and communication.

INTRODUCTION

Spectroscopy of atoms and molecules supports studies of quantum matter and numerous applications. An important advance in laser spectroscopy and metrology has been the use of optical-frequency combs (*1*, *2*). Specifically, combs can interact with atoms and molecules in direct frequency comb spectroscopy (DFCS), providing conceptually important measurements (*3*, *4*). In recent years, DFCS has been applied to demonstrate sensitive and broadband molecular spectroscopy (*5*, *6*), breath analysis (*7*), precision atomic spectroscopy (*8*–*10*), steering Raman transitions (*11*), atomic clocks, (*12*) Ramsey spectroscopy (*13*), temperature sensing (*14*), and extreme ultraviolet spectroscopy (*15*), using numerous techniques such as dual-comb spectroscopy, cavity-enhanced spectroscopy, fluorescence, and Ramsey spectroscopy. Such a wide range of application directions and techniques are enabled by robust and controllable frequency comb sources.

Recently, dissipative Kerr solitons in optical microresonators have been demonstrated to provide a compact platform for low-noise, microwave-rate, and low–power frequency combs (*16*). Pumped with a continuous laser, stable soliton pulses can be generated in a Kerr-nonlinear microresonator. Despite the vast progress in using DFCS in table-top combs, so far, demonstrations of microcomb-based DFCS have been mainly focused in gigahertz-linewidth molecular spectroscopy (*6*, *17*). Thus, the question of how to precisely control and directly interface microcombs with an atomic medium remains unresolved. Soliton microcombs have already been used for various applications (*16*), where for most, it is essential to leverage precise frequency control of the soliton mode spectrum $\nu_m = f_{ceo} + m \cdot f_{rep}$ through two degrees of freedom, i.e., the repetition frequency f_{rep} and the carrier-envelope offset frequency f_{ceo}. However, these parameters are coupled together in a complex manner by the soliton dynamics; this was determined in (*18*) for high-Q silica microresonators. Through the so-called "fixed points" of a microcomb, the possibility exists to decouple and precisely control f_{rep} and f_{ceo}. We can use this feature for high-resolution microcomb DFCS. A second approach is to stabilize f_{rep}, using phase modulation of the microcomb pump laser at the free-spectral range (FSR). This technique was explored in (*19*), and we can use it in DFCS to define a constant f_{rep} with respect to a microwave clock, which completely decouples f_{ceo} from f_{rep} and allows substantial scanning and stabilization. A parallel benefit of microcomb DFCS is to derive a compact, low-power, and stable frequency comb spectrum by stabilization to a DFCS signal. Different avenues of frequency stabilization microcombs have been explored, including microcombs locked to a table-top frequency comb system (*20*), all optical double-pinning methods (*21*), and optical locking of a frequency-doubled mode of a Kerr resonator to an atomic transition (*22*). Such approaches often require multiple helper lasers and nonlinear crystals that produce a large footprint. A microcomb-based frequency comb directly interfaced to a compact atomic medium may serve the vision to construct a fully chip scale–stable optical ruler. Recent advances in integrated photonic-atomic systems (*23*, *24*) may further support such highly compact physics package.

Here, we demonstrate microcomb DFCS of the cascaded $5P_{3/2}$-$4D_{5/2}$ transition in ^{85}Rb at 1529.37 nm. By demonstrating our ability to physically decouple between the microcomb's degrees of freedom in the frequency domain, we are capable of performing high-precision microcomb–based atomic spectroscopy and stabilization with megahertz-level resolution and kilohertz-level stability. This telecom-wavelength band atomic transition is convenient and unique given the technological advantage of operating microcombs with telecom lasers and other components. We generate a soliton microcomb with a 1536-nm phase-modulated (PM) pump laser and use one microcomb mode to interact with Rb atoms in a micromachined vapor cell (*25*). By also probing the near-infrared Rb D2 transition at 780 nm with a second laser, we resolve the dipole-allowed $4^2D_{5/2}$ hyperfine manifold composed of ~10-MHz linewidth

[1]Time and Frequency Division, National Institute for Standards and Technology, Boulder, CO 80305, USA. [2]Department of Physics, University of Colorado Boulder, Boulder, CO 80309, USA. [3]T. J. Watson Laboratory of Applied Physics, California Institute of Technology, Pasadena, CA 91125, USA.
*Corresponding author. Email: liron.stern@mail.huji.ac.il (L.S.); scott.papp@nist.gov (S.B.P)

atomic transitions. This double-resonance optical pumping (DROP) technique (*26*–*28*) not only enables an enhancement in signal-to-noise ratio with DFCS but also circumvents photodiode background noise from modes of the microcomb that are off-resonance of rubidium transitions. By frequency-locking the microcomb f_{ceo} to the $F = 4$–to–$F' = 3$ hyperfine transition among the $4^2D_{5/2}$ manifold, we stabilize the fractional-frequency noise at the 10^{-11} level. Moreover, we perform a day-to-day accuracy assessment, which indicates a <1-MHz repeatability in the absolute f_{ceo} of the microcomb. The microcomb DFCS technique that we describe is a general, robust, and compact approach to implement an atomic transition–referenced microcomb, and it could be expanded to other spectral ranges and to multiphoton DFCS.

RESULTS

Figure 1 presents an overview of our apparatus and results. We generate a soliton microcomb with a silica resonator that is evanescently coupled via a tapered fiber (*29*); see the schematic in Fig. 1A. The resonator is pumped with a 1536-nm laser, and the generated soliton microcomb spectrum extends approximately 60 nm across the telecom C-band. For microcomb DFCS, we send the soliton microcomb light into a Rb atomic vapor. We implement the microcomb-atom interaction via a pump-probe DROP scheme, involving one mode of the microcomb and a 780-nm laser; the atomic level diagram is depicted in the inset of Fig. 1A. The DROP approach is an optical spectroscopic pump-probe technique implemented in a ladder three-level atomic system, which detects the ground state to intermediate level absorption as a probe for intermediate to excited-state population. In our system, the 5^2S ground state $F = 3$ hyperfine state is primarily coupled to the $5^2P_{3/2}$ $F = 3$ cycling transition. This is achieved by using the D2 transition at 780 nm, which acts as a probe. A second transition at the telecom wavelength of 1529 nm couples the $5^2P_{3/2}$ state to the $4^2D_{5/2}$ hyperfine manifold and acts as an atomic pump (distinct from the frequency comb pump). The DROP technique has a few prominent advantages for implementation in DFCS. First, this pump-probe arrangement allows us to imprint the spectroscopic information of the telecom hyperfine manifold on the 780-nm probe. Moreover, by nature of the optical-pumping process (i.e., transfer of atomic population between the two 5^2S ground states), we gain a substantial increase in signal due to decrease in population in the upper 5^2S state (*27*). Consequently, the spectrum will consist of three peaks. The width of these peaks is limited by the excited state and intermediate states lifetimes and is essentially Doppler free because of the combination of velocity selection processes and two-photon coherence effects (*27*, *30*). These features make the cascaded atomic system appealing for implementation of DFCS (*31*). Figure 1B shows the devices that we use, namely, a high-*Q* silica wedge resonator on a silicon chip and a micromachined, dispenser-based Rb atomic vapor cell.

We create the soliton microcomb by pumping the silica resonator with a 1536-nm external-cavity diode laser (ECDL). Direct, deterministic single-soliton pulses are generated by pumping the microresonator with 100 mW of PM light (*19*); the PM frequency is derived from a hydrogen maser–referenced microwave synthesizer that is set close (with a bandwidth of 80 kHz) to the resonator's FSR of ~22 GHz. With the PM light engaged, the microcomb's f_{rep} is tightly locked to the PM frequency. An illustration of this process is also shown in Fig. 1A. This PM technique allows us to initiate single solitons without transitioning through the chaotic regime. Moreover, seeding the comb with the PM frequency forces the repetition rate of the comb to align with the seeding frequency and directly controls and decouple f_{rep} from f_{ceo}. The optical-frequency spectrum is presented in Fig. 1C, where a comb spanning across the C-band is evident, as well as the seeding PM light. A zoomed section shows the specific comb mode that interacts with the atomic medium.

We use microcomb f_{ceo} tuning to acquire the DFCS signal of the cascaded Rb transitions. Operationally, we change the pump-laser power to exclusively tune f_{ceo}, but this requires a detailed two-part microcomb control procedure. First, we rely on the PM pumping

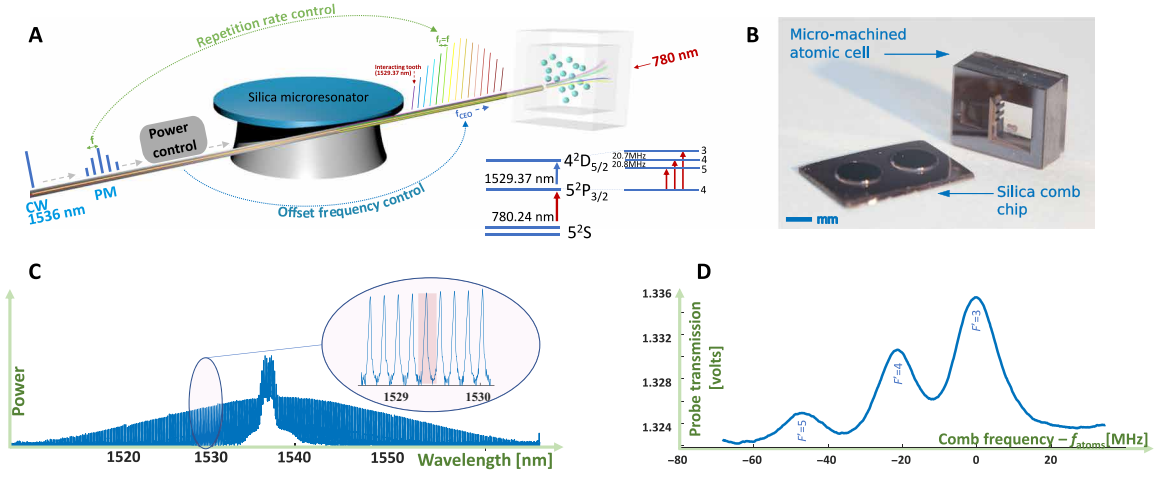

Fig. 1. Direct Kerr comb atomic spectroscopy. (**A**) Conceptual depiction of the microcomb and atomic system. A PM and power-controlled 1536-nm pump laser energizes a single-soliton pulse in a silica whispering galley–mode resonator. The power control and phase-modulation frequency discipline f_{rep} and f_{ceo}, respectively. The comb spectrum, in turn, illuminates a millimeter-scale micromachined rubidium cell. The comb has a 1529-nm mode that is resonant with a ^{85}Rb two-step atomic transition; see relevant Rb atomic-level scheme in inset. (**B**) Photograph of typical Kerr comb chip and micromachined Rb vapor cell. (**C**) Soliton microcomb optical spectrum acquired with 20-pm resolution; zoomed section highlights the mode that interacts with the atomic medium. (**D**) Probe transmission signal as function of comb frequency, revealing the $4^2D_{5/2}$ dipole-allowed hyperfine manifold. Photo credit: Liron Stern, NIST (B).

technique to maintain a fixed value of f_{rep}. Second, we stabilize the frequency detuning of the pump laser with respect to the silica resonance, using an offset Pound-Drever-Hall (PDH) technique (*18*). Stabilizing the frequency detuning both allows precise control of the actual value of the detuning and eliminates the f_{ceo} dependence on frequency detuning fluctuations. Changing the pump-laser power causes thermal and nonlinear shifts of the silica resonance and induces an exclusive shift in f_{ceo} of the entire equidistant comb, which we use for Rb DFCS. The spectroscopy data of the Rb transitions obtained with an approximately 50% change in the microcomb pump power are presented in Fig. 1D. Specifically, the 1529-nm comb mode induces a variation in the 780-nm probe laser transmission through the Rb vapor cell. Three clear peaks (as anticipated from the DROP nature of this process) are evident, corresponding to the three dipole-allowed transitions from the $5P_{3/2}$ $F = 4$ state to the $4D_{5/2}$ 3,4,5 states. The linewidth is measured to be ~10 MHz, which is close to the limit of 6 MHz imposed by velocity selection and two-photon coherence processes (*27*, *30*). To the best of our knowledge, this is the first report resolving a hyperfine spectroscopic feature with megahertz-level resolution directly using Kerr combs.

The ability to decouple the microcomb's physical controls, i.e., pump-laser power and frequency, and the resonator detuning, from the microcomb's degrees of freedom, i.e., f_{ceo} and f_{rep}, is central to the implementation of high-resolution DFCS and subsequent stabilization. The coupling of these parameters arises in a complex manner from frequency shifts of the thermo-optic effect, the Kerr effect, and the self-soliton effect that all act simultaneously. Therefore, a key question is to what extent our microcomb operation procedure, which is shown conceptually in Fig. 2A (an elaborate description of this procedure is introduced in fig. S1), achieves such decoupling. To answer this, we carry out an experiment in which we scan f_{ceo} and monitor f_{rep} with a microwave frequency–counting system. For microwave counting, we select only a portion of the comb separate from the PM pump modes. We present such a measurement in Fig. 2B for two different scenarios; the black- and blue-colored traces indicate f_{rep}, and the orange trace is the pump power. In the first scenario, the pump power is kept constant, and the f_{rep} data indicate a stable lock. In the second scenario, the power is varied periodically, with an amplitude corresponding to a 50% change, but f_{rep} remains unchanged, indicating the robustness of the locking. To compare the scenarios in detail, we record a more extensive frequency-counter dataset and calculate the overlapping Allan deviation; see Fig. 2C. Here, the Allan deviation averages down as τ^{-1}, indicating that the microcomb f_{rep} is effectively locked to the synthesizer's frequency f and that the nonlinear processes do not write additional noise on f_{rep} even when f_{ceo} is perturbed. When we abruptly vary the pump power, we do not observe a change in the locked accuracy or precision of the soliton microcomb repetition frequency. These data confirm the capability to decouple f_{ceo} and f_{rep}, solving an important challenge for high-precision soliton microcomb DFCS. By recognizing that such power variation induces the spectroscopy presented in Fig. 1D, we conclude that the soliton pulse envelope remains intact while independently controlling underlying carrier wave.

We demonstrate one specific use of microcomb DFCS: stabilization of the absolute optical frequency of the entire set of comb teeth. In this experiment, we maintain the repetition-frequency stability using PM pumping and its feeding synthesizer as described above and stabilize f_{ceo} using the direct interface with the atomic medium. To implement a servo lock of f_{ceo}, with respect to the DFCS signal,

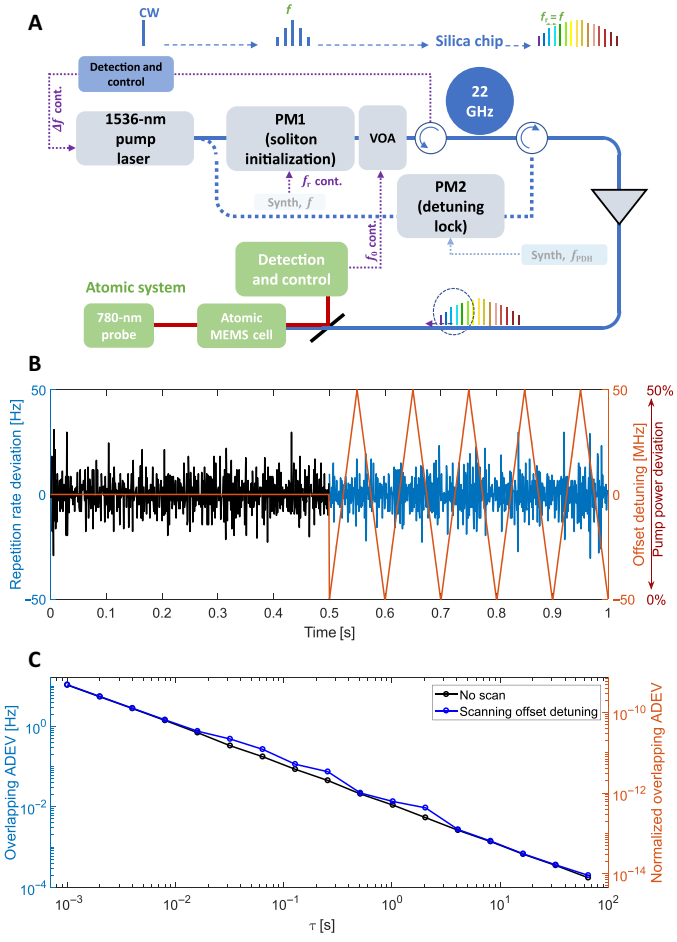

Fig. 2. DFCS apparatus and demonstration of f_{rep} control. (**A**) An ECDL drives frequency shifter, driven by a voltage-controlled oscillator (VCO). The pump beam is PM (PM1) at FSR. We implement a PDH servo-loop to control the resonator detuning with a counterpropagating PM (PM2) beam. This counterpropagating beam is circulated and detected to create an error signal and control the pump frequency. A portion of the comb spectrum is amplified and sent to a micromachined atomic cell, which is also illuminated by a counterpropagating continuous wave (CW) 780-nm probe laser. By using a dichroic mirror and a Si photodetector, the 780-nm light is monitored to create an error signal to control a variable optical attenuator to lock f_{ceo} to the atomic transition. (**B**) Soliton microcomb f_{rep} and pump power setting versus time (red). Blue and black f_{rep} data indicate the different power conditions. (**C**) Corresponding overlapping Allan deviation (ADEV) for the case of constant and swept pump power.

we dither the pump-laser power to obtain an error signal and use a proportional–integral–derivative (PID) controller to provide feedback. The variable optical attenuator indicated in Fig. 2A provides the dither. Stabilization of the microcomb via the DROP spectroscopy technique also requires that the 780-nm probe laser is stabilized to the Rb D2 transition. In this work, we accomplish the 780-nm laser stabilization in a separate saturated absorption apparatus, but this could, in principle, also be performed in the same micromachined cell as the DROP spectroscopy.

We characterize the frequency stability of the Rb-referenced microcomb by frequency-counting a specific tooth (a few modes apart in frequency from the pump frequency), with respect to a self-referenced erbium-fiber frequency comb (*32*). In Fig. 3A, we present the overlapping Allan deviation of the microcomb with Rb stabilization (red points) and without (blue points). By referencing the microcomb to

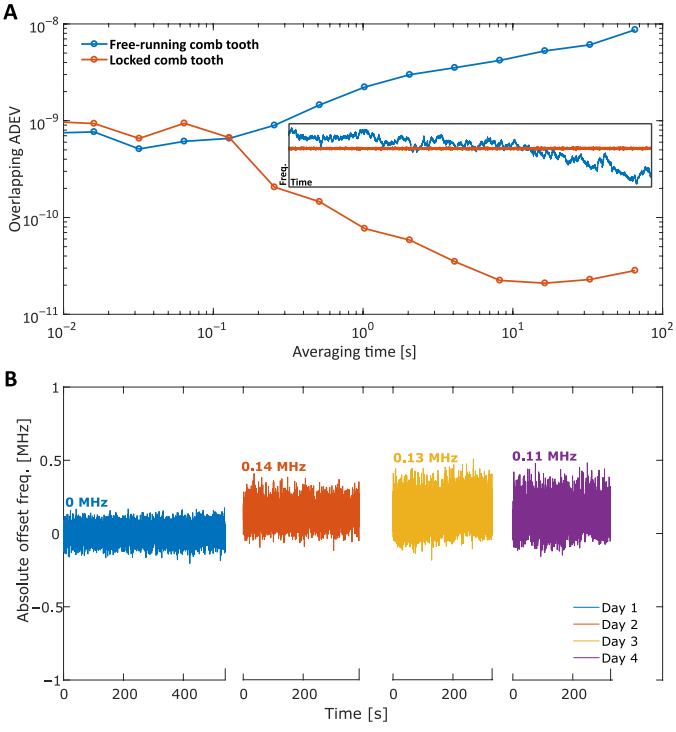

Fig. 3. Direct Kerr comb atomic stabilization and day-to-day accuracy. (**A**) Uncertainty assessment of the optical frequency precision represented by an overlapping Allan deviation plot for the locked (red) and unlocked case (blue). The inset shows the time domain data over ~10 min from which the Allan deviation is calculated. (**B**) Day-to-day optical frequency traces obtained by reinitiating the Kerr comb and locking the comb directly to the cascaded atomic transition.

the hyperfine structure of Rb, we improve its fractional-frequency stability to as low as 2×10^{-11} after 10 s of measurement time. Therefore, with our system, all the microcomb mode frequencies are stable at the ~10-kHz level.

A potentially more important benefit of atomic-Rb stabilization of our 1550-nm-band soliton microcomb is the long-term repeatability of the microcomb mode frequencies. In this manner, a microcomb could be available for an application without need for recalibration or alignment. To assess day-to-day repeatability, we operate the system over a span of 4 days, each day restarting the microcomb and Rb laser system components, initiate a soliton microcomb, tune the microcomb into resonance of the Rb transition, apply the stabilization, and count the optical frequency. We leave the Rb temperature stabilization running at all times. We present these results in Fig. 3B, where each optical-frequency trace (indicated by different colors) represents a frequency measurement performed on a separate day. The maximum day-to-day frequency change is 140(4) kHz (from the first day to second), and the SD of the shifts is 65(4) kHz. The absolute deviation corresponds to fractional uncertainty of 7×10^{-10}, and the last 3 days are a bit better. Considering that the system is subject to environmental perturbations, is unshielded from magnetic fields, and is not packaged, it would likely be possible to improve upon this performance. And yet, for the given system, such accuracies and stability already support applications such as chip-scale–based dimensional spectroscopy, hazardous material sensing, and wavelength meter calibration. Moreover, when considering a miniaturized system, such demonstrated level of performance for stabilization of f_{rep} is consistent with commercial Rb microwave references and crystal oscillators. For instance, considering a commercial oven-compensated crystal oscillator, capable of short-time stability and accuracy at the 10^{-12} and 10^{-8} level, respectively, would allow frequency stabilities at the level demonstrated above for a bandwidth of ~50 nm (corresponding to ~300 modes).

DISCUSSION

To summarize, we have demonstrated direct Kerr-microcomb atomic spectroscopy by exploiting the cascaded $5P_{3/2}$-$4D_{5/2}$ transition in ^{85}Rb. We use a comb mode near the $5P_{3/2}$-$4D_{5/2}$ transition frequency to interact with the ^{85}Rb atoms by sending most of the comb spectrum directly into the micromachined vapor cell. Our spectroscopy experiments are enabled by fine frequency control of the microcomb, which allows us to resolve the closely spaced hyperfine manifold with linewidths of ~10 MHz. Even higher-resolution spectroscopy is possible because of continuous sweeping of the microcomb. By implementing a servo-loop, we lock the comb to the $5^2P_{3/2}$ $F = 4$ state–to–$4^2D_{5/2}$ $F' = 3$ state atomic transition with a frequency uncertainty approaching 10^{-11}. Accuracy assessment of the system shows a sub-megahertz accuracy over a few days. Such level of performance in a compact footprint is competitive with previous demonstrations stabilizing soliton Kerr-combs. Moreover, leveraging this level of accuracy to use the same comb to perform direct and traceable spectroscopy on a different atomic specimen is possible by tuning the synthesizer while maintaining the atomic lock. Our ability to decouple f_{rep} and f_{ceo} may further allow to demonstrate multiphoton excitations, such as the 778-nm two-photon absorption transition in Rb (*33*) and allow to interact directly with hyperfine transitions in atoms (*34*, *35*) via Raman transitions or electromagnetic-induced transparency. These realizations may allow to fully optically stabilize a Kerr comb to an atomic medium and pave the way to other exciting Kerr-based DFCS experiments.

MATERIALS AND METHODS

PM soliton initiation

The ECDL was driving a single-sideband (SSB), suppressed-carrier frequency modulator controlled by a high-bandwidth voltage-controlled oscillator (VCO) for control of the pump laser. A portion of the laser was frequency shifted and modulated by means of an acousto-optic modulator and PM, whereas one sideband of the PM light was locked to the cavity resonance. The high-bandwidth feedback allowed by the VCO/SSB scheme allowed thermal instabilities associated with the red detuning that is required for soliton generation to be overcome. A counterpropagating (with respect to the acousto-optic modulator–shifted beam) PM pump beam was coupled to the resonator, thus parametrically seeding the resonator and allowing deterministic creation of single solitons. To generate single solitons, the pump laser was initially detuned ~25 linewidths from resonance, and subsequently, the detuning was decreased to ~3 linewidths, where a soliton step was observed. An elaborate schematic of the experimental arrangement is presented in fig. S1.

Micromachined vapor cell fabrication

The vapor cell has been constructed by using a combination of wafer-scale fabrication silicon frames, anodic bonding, and Rb dispenser pills (*25*). First, a 3-mm-thick silicon wafer was structured using a

deep reactive-ion etching process, to create a silicon frame with two chambers connected by channels. The large chamber has the dimensions of 3 mm by 3 mm, whereas the small chamber has the dimension of 1.5 mm by 1.5 mm. Next, a 0.7-mm-thick Pyrex window was anodically bonded to the silicon frame to form a preform. Following, in a vacuum environment, a Rb dispenser pill was introduced in the small enclosure, and a second Pyrex window was anodically bonded to the exposed side of the silicon frame, creating a closed cell. Last, the cell was activated by illuminating the dispenser pill with approximately 1 W of 980-nm laser power to release natural rubidium into the chambers enclosed within the cell.

Spectroscopy and stabilization setup

The rubidium spectroscopy setup was based on the two-photon cascaded transition in ^{85}Rb. A 780-nm ECDL was locked to the $F = 2$–to–$F' = 3$ D2 transition in a centimeter-scale rubidium cell using saturation spectroscopy. The frequency uncertainty of this laser characterized by comparing its frequency to a commercial frequency comb is $3 \times 10^{-12}/\tau^{1/2}$. The laser was sent over fiber to illuminate the millimeter-scale micro-machined cell with a beam diameter of approximately 1 mm. This laser serves as a probe for the counter-propagating Kerr comb light interacting with the atoms. The Kerr comb has an approximate beam diameter of 900 μm, and the interacting comb mode has an amplified power of approximately 50 μW. The Kerr comb was stabilized to the cascaded transition by feeding the variable optical attenuator (VOA) with approximately 500-Hz demodulated error signal. Last, a mode close to the pump frequency is filtered out, compared to a tooth of the commercial locked frequency comb system, and frequency was counted. Through a separate systematic characterization of the DROP atomic transition, using a telecom ECDL, we assessed two dominant contributions to frequency shifts in our system: variations in the cell temperature and optical power of the atomic system's pump and probe. This analysis shows that our cell has a normalized frequency temperature coefficient of 10^{-10}/°C and a frequency power coefficient of $\sim 2 \times 10^{-11}$ and $\sim 8 \times 10^{-11}$ for a change of 1% of the 780- and 1529-nm powers, respectively. These coefficients allow the stability performance levels reported here to be reached without any stringent temperature or power stabilization control.

SUPPLEMENTARY MATERIALS

Supplementary material for this article is available at http://advances.sciencemag.org/cgi/content/full/6/9/eaax6230/DC1

Fig. S1. Kerr comb DFCS elaborate apparatus.

REFERENCES AND NOTES

1. J. L. Hall, Nobel lecture: Defining and measuring optical frequencies. *Rev. Mod. Phys.* **78**, 1279–1295 (2006).
2. T. W. Hänsch, Nobel lecture: Passion for precision. *Rev. Mod. Phys.* **78**, 1297–1309 (2006).
3. M. C. Stowe, M. J. Thorpe, A. Pe'er, J. Ye, J. E. Stalnaker, V. Gerginov, S. A. Diddams, Direct frequency comb spectroscopy. *Adv. At. Mol. Opt. Phys.* **55**, 1–60 (2008).
4. A. Marian, M. C. Stowe, J. R. Lawall, D. Felinto, J. Ye, United time-frequency spectroscopy for dynamics and global structure. *Science* **306**, 2063–2068 (2004).
5. B. Bernhardt, A. Ozawa, P. Jacquet, M. Jacquey, Y. Kobayashi, T. Udem, R. Holzwarth, G. Guelachvili, T. W. Hänsch, N. Picqué, Cavity-enhanced dual-comb spectroscopy. *Nat. Photonics* **4**, 55–57 (2010).
6. M. Yu, Y. Okawachi, C. Joshi, X. Ji, M. Lipson, A. L. Gaeta, Gas-phase microresonator-based comb spectroscopy without an external pump laser. *ACS Photonics* **5**, 2780–2785 (2018).
7. M. J. Thorpe, D. Balslev-Clausen, M. S. Kirchner, J. Ye, Cavity-enhanced optical frequency comb spectroscopy: Application to human breath analysis. *Opt. Express* **16**, 2387–2397 (2008).
8. M. C. Stowe, F. C. Cruz, A. Marian, J. Ye, High resolution atomic coherent control via spectral phase manipulation of an optical frequency comb. *Phys. Rev. Lett.* **96**, 153001 (2006).
9. D. C. Heinecke, A. Bartels, T. M. Fortier, D. A. Braje, L. Hollberg, S. A. Diddams, Optical frequency stabilization of a 10 GHz Ti:sapphire frequency comb by saturated absorption spectroscopy in ^{87}rubidium. *Phys. Rev. A* **80**, 053806 (2009).
10. I. Barmes, S. Witte, K. S. E. Eikema, High-precision spectroscopy with counterpropagating femtosecond pulses. *Phys. Rev. Lett.* **111**, 023007 (2013).
11. C. Solaro, S. Meyer, K. Fisher, M. V. DePalatis, M. Drewsen, Direct frequency-comb-driven raman transitions in the terahertz range. *Phys. Rev. Lett.* **120**, 253601 (2018).
12. V. Gerginov, C. E. Tanner, S. A. Diddams, A. Bartels, L. Hollberg, High-resolution spectroscopy with a femtosecond laser frequency comb. *Opt. Lett.* **30**, 1734 (2005).
13. J. Morgenweg, I. Barmes, K. S. E. Eikema, Ramsey-comb spectroscopy with intense ultrashort laser pulses. *Nat. Phys.* **10**, 30–33 (2014).
14. A. Klose, G. Ycas, F. C. Cruz, D. L. Maser, S. A. Diddams, Rapid, broadband spectroscopic temperature measurement of CO_2 using VIPA spectroscopy. *Appl. Phys. B* **122**, 78 (2016).
15. A. Cingöz, D. C. Yost, T. K. Allison, A. Ruehl, M. E. Fermann, I. Hartl, J. Ye, Direct frequency comb spectroscopy in the extreme ultraviolet. *Nature* **482**, 68–71 (2012).
16. T. J. Kippenberg, A. L. Gaeta, M. Lipson, M. L. Gorodetsky, Dissipative Kerr solitons in optical microresonators. *Science* **361**, eaan8083 (2018).
17. M. Yu, Y. Okawachi, A. G. Griffith, M. Lipson, A. L. Gaeta, Microresonator-based high-resolution gas spectroscopy. *Opt. Lett.* **42**, 4442–4445 (2017).
18. J. R. Stone, T. C. Briles, T. E. Drake, D. T. Spencer, D. R. Carlson, S. A. Diddams, S. B. Papp, Thermal and nonlinear dissipative-soliton dynamics in Kerr-microresonator frequency combs. *Phys. Rev. Lett.* **121**, 063902 (2018).
19. D. C. Cole, J. R. Stone, M. Erkintalo, K. Y. Yang, X. Yi, K. J. Vahala, S. B. Papp, Kerr-microresonator solitons from a chirped background. *Optica* **5**, 1304–1310 (2018).
20. P. Del'Haye, O. Arcizet, A. Schliesser, R. Holzwarth, T. J. Kippenberg, Full stabilization of a microresonator-based optical frequency comb. *Phys. Rev. Lett.* **101**, 053903 (2008).
21. S. B. Papp, K. Beha, P. Del'Haye, F. Quinlan, H. Lee, K. J. Vahala, S. A. Diddams, Microresonator frequency comb optical clock. *Optica* **1**, 10–14 (2014).
22. W. Liang, A. A. Savchenkov, V. S. Ilchenko, D. Eliyahu, A. B. Matsko, L. Maleki, Stabilized C-band Kerr frequency comb. *IEEE Photonics J.* **9**, 1–11 (2017).
23. L. Stern, B. Desiatov, I. Goykhman, U. Levy, Nanoscale light–matter interactions in atomic cladding waveguides. *Nat. Commun.* **4**, 1548 (2013).
24. M. T. Hummon, S. Kang, D. G. Bopp, Q. Li, D. A. Westly, S. Kim, C. Fredrick, S. A. Diddams, K. Srinivasan, V. Aksyuk, J. E. Kitching, Photonic chip for laser stabilization to an atomic vapor with 10^{-11} instability. *Optica* **5**, 443–449 (2018).
25. L.-A. Liew, S. Knappe, J. Moreland, H. Robinson, L. Hollberg, J. Kitching, Microfabricated alkali atom vapor cells. *Appl. Phys. Lett.* **84**, 2694–2696 (2004).
26. H. S. Moon, W. K. Lee, L. Lee, J. B. Kim, Double resonance optical pumping spectrum and its application for frequency stabilization of a laser diode. *Appl. Phys. Lett.* **85**, 3965–3967 (2004).
27. H. S. Moon, L. Lee, J. B. Kim, Double-resonance optical pumping of Rb atoms. *J. Opt. Soc. Am. B* **24**, 2157–2164 (2007).
28. H. S. Moon, W.-K. Lee, H. S. Suh, Hyperfine-structure-constant determination and absolute-frequency measurement of the Rb $4D_{3/2}$ state. *Phys. Rev. A* **79**, 062503 (2009).
29. X. Yi, Q.-F. Yang, K. Y. Yang, M.-G. Suh, K. Vahala, Soliton frequency comb at microwave rates in a high-Q silica microresonator. *Optica* **2**, 1078–1085 (2015).
30. M. Tanasittikosol, C. Carr, C. S. Adams, K. J. Weatherill, Subnatural linewidths in two-photon excited-state spectroscopy. *Phys. Rev. A* **85**, 033830 (2012).
31. H. S. Moon, H. Y. Ryu, S. H. Lee, H. S. Suh, Precision spectroscopy of Rb atoms using single comb-line selected from fiber optical frequency comb. *Opt. Express* **19**, 15855–15863 (2011).
32. G. Ycas, S. Osterman, S. A. Diddams, Generation of a 660–2100 nm laser frequency comb based on an erbium fiber laser. *Opt. Lett.* **37**, 2199–2201 (2012).
33. S. Y. Zhang, J. T. Wu, Y. L. Zhang, J. X. Leng, W. P. Yang, Z. G. Zhang, J. Y. Zhao, Direct frequency comb optical frequency standard based on two-photon transitions of thermal atoms. *Sci. Rep.* **5**, 15114 (2015).
34. D. Hayes, D. N. Matsukevich, P. Maunz, D. Hucul, Q. Quraishi, S. Olmschenk, W. Campbell, J. Mizrahi, C. Senko, C. Monroe, Entanglement of atomic qubits using an optical frequency comb. *Phys. Rev. Lett.* **104**, 140501 (2010).
35. D. Hou, J. Wu, S. Zhang, Q. Ren, Z. Zhang, J. Zhao, A stable frequency comb directly referenced to rubidium electromagnetically induced transparency and two-photon transitions. *Appl. Phys. Lett.* **104**, 111104 (2014).

Acknowledgments: We thank S.-P. Yu and M. Hummon for comments on the manuscript. We acknowledge the Kavli Nanoscience Institute. This work is a contribution of the U.S. government and is not subject to copyright in the United States. **Funding:** We acknowledge funding from DARPA DODOS and ACES programs, NASA, AFOSR award number FA9550-16-1-0016, and NIST. **Author contributions:** L.S. conceived the concept and analyzed the data. L.S.

and J.R.S. performed the experiments and wrote the paper. D.C.C. contributed to develop the phase modulation initialization technique. Z.N., M.-G.S., J.K., and K.V. contributed to fabrication of the devices. S.K. and J.K. provided the Rb-stabilized reference laser. C.F. and S.A.D. provided the frequency comb reference system. S.B.P. supervised the project, designed the experiments, and wrote the paper. **Competing interests:** The authors declare that they have no competing interests. **Data and materials availability:** All data needed to evaluate the conclusions in the paper are present in the paper and/or the Supplementary Materials. Additional data related to this paper may be requested from the authors.

Submitted 8 April 2019
Accepted 5 December 2019
Published 28 February 2020
10.1126/sciadv.aax6230

Citation: L. Stern, J. R. Stone, S. Kang, D. C. Cole, M.-G. Suh, C. Fredrick, Z. Newman, K. Vahala, J. Kitching, S. A. Diddams, S. B. Papp, Direct Kerr frequency comb atomic spectroscopy and stabilization. *Sci. Adv.* **6**, eaax6230 (2020).